A novel variant fibrinogen, AαE11del, demonstrating the importance of AαE11 residue in thrombin binding

Takahiro Kaido[a,b], Masahiro Yoda[c], Tomu Kamijo[a,b], Shinpei Arai[c], Kazuyoshi Yamauchi[c], Nobuo Okumura[c,d]

[a] Department of Medical Sciences, Graduate School of Medicine, Science and Technology, Shinshu University, Matsumoto, Japan
[b] Department of Laboratory Medicine, Shinshu University Hospital, Matsumoto, Japan
[c] Department of Clinical Laboratory Investigation, Graduate School of Medicine, Shinshu University, Matsumoto, Japan
[d] Laboratory of Clinical Chemistry and Immunology, Department of Biomedical Laboratory Sciences, School of Health Sciences, Shinshu University, Matsumoto, Japan

Running head: AαE11 play a key role in thrombin binding
Type of manuscript: original article

Address correspondence to:
Nobuo Okumura, Ph.D. Laboratory of Clinical Chemistry and Immunology
Department of Biomedical Laboratory Sciences
School of Health Sciences
Shinshu University
3-1-1 Asahi, Matsumoto 390-8621, Japan
Tel.: 81-263-37-2392
Fax: 81-263-37-2370
E-mail: nobuoku@shinshu-u.ac.jp

Word count: 4709
Abstract:199
Figures: 4
Tables: 2
Supplementary Figure: 1
References: 35

Abstract

Introduction: We identified a novel heterozygous AαE11del variant in a patient with congenital dysfibrinogenemia. This mutation is located in fibrinopeptide A (FpA). We analyzed the effect of AαE11del on the catalyzation of thrombin and batroxobin and simulated the stability of the complex structure between the FpA fragment (AαG6-V20) peptide and thrombin.

Materials and Methods: We performed fibrin polymerization and examined the kinetics of FpA release catalyzed by thrombin and batroxobin using purified plasma fibrinogen. To clarify the association between the AαE11 residue and thrombin, we calculated binding free energy using molecular dynamics simulation trajectories.

Results: Increasing the thrombin concentration improved release of FpA from the patient's fibrinogen to approximately 90%, compared to the previous 50% of that of normal fibrinogen. Fibrin polymerization of variant fibrinogen also improved. In addition, greater impairment of variant FpA release from the patient's fibrinogen was observed with thrombin than with batroxobin. Moreover, the calculated binding free energy showed that the FpA fragment–thrombin complex became unstable due to the missing AαE11 residue.

Conclusions: Our findings indicate that the AαE11 residue is involved in FpA release in thrombin catalyzation more than in batroxobin catalyzation, and that the AαE11 residue stabilizes FpA fragment–thrombin complex formation.

Keywords: binding free energy; dysfibrinogenemia; fibrinogen; fibrinopeptide A; thrombin

Introduction

Fibrinogen is a 340 kDa plasma glycoprotein composed of two sets of three different polypeptide chains (Aα: 610, Bβ: 461, and γ: 411 residues) [1], which are encoded by three genes: *FGA*, *FGB*, and *FGG*, respectively [2]. Two sets of these polypeptides combine at each N-terminal portion and form a symmetrical trinodular molecule consisting of a central E region and two distal D regions through a link with triple helix coiled-coil connectors [3,4].

The enzymes that convert fibrinogen into fibrin are serine-type proteases such as thrombin or batroxobin (snake venom protease from *Bothrops atrox*). Thrombin releases fibrinopeptide A (FpA; AαA1-R16 residues) and fibrinopeptide B (FpB; BβQ1-R14 residues) from the N-terminus of the Aα-chains and the Bβ-chains, respectively [5], whereas batroxobin releases only FpA [6]. Fibrin clot formation starts with the formation of half-staggered, double-stranded protofibrils by FpA release [2].

The active site of thrombin binds to fibrinogen AαD7-R19 residues [7]. A number of amino acid substitutions in AαD7-R19 residues have been reported and listed on the Groupe d'etude sur l'hemostase et la thrombose (GEHT) homepage, and all of them have been reported to show dysfibrinogenemia [8]. Part of the FpA structure with one turn of a helix (residues AαD7-E11) and a type I β-turn (residues AαL9-G12) has been revealed by X-ray crystallography [9].

In this study, we identified a novel variant fibrinogen associated with dysfibrinogenemia. Because this mutation was located inside the FpA, we compared differences in fibrin polymerization and FpA release properties between normal and variant fibrinogen using purified plasma fibrinogen. In addition, we analyzed individual residues internal to FpA for FpA–thrombin binding using molecular dynamics (MD) simulation.

Materials and methods

This study was approved by the Ethics Review Board of Shinshu University School of Medicine (approval number 603). After informed consent had been obtained from the propositus, blood samples were collected for biochemical and genetic analyses. Amino acid numbers of fibrinogen are shown according to the mature protein numbering, and that of thrombin is indicated by chymotrypsinogen numbering of bovine trypsin.

Coagulation screening tests and DNA sequencing of the fibrinogen gene

Blood collection from propositus and plasma separation were performed, and prothrombin time (PT), activated partial thromboplastin time (APTT), and fibrinogen concentrations were measured as described previously [10].

To amplify all exons and exon–intron boundaries in the fibrinogen gene, polymerase chain reaction (PCR) primers were designed and DNA was amplified using PCR, and the PCR

products were purified from agarose gels as described previously [11]. Purified PCR products were directly sequenced as described previously [10]. In the case of insertions and/or deletions, the region was amplified using PCR, and PCR products were cloned using a TOPO TA Cloning Kit for Sequencing (Invitrogen, Waltham, MA, USA). Then, the cloned products were sequenced as described above.

Purification of plasma fibrinogen

Purification of plasma fibrinogen from a healthy person and the propositus was performed using immunoaffinity chromatography with an IF-1 monoclonal antibody (LSI Medience, Tokyo, Japan)-conjugated Sepharose 4B column [12,13], and purified fibrinogen concentrations were determined from the $\Delta Abs_{280\text{-}320}$ on the assumption that 1 mg/mL gives a result of 1.51 [14]. The purity and characterization of each purified fibrinogen was analyzed by sodium dodecyl sulfate-polyacrylamide gel electrophoresis (SDS-PAGE) in reducing conditions (10% gel) or non-reducing conditions (5% gel) and stained with Coomassie Brilliant Blue R-250.

Thrombin- or batroxobin-catalyzed fibrin polymerization

Turbidity curves of fibrin polymerization were recorded at 350 nm using a UV-1280 (Shimadzu, Tokyo, Japan). Recordings were performed in a final volume of 100 μL as described

previously [10], with a few minor modifications. Briefly, 10 μL of human α-thrombin (Enzyme Research Laboratories, South Bend, MA, USA, 0.5 U/mL or 40 U/mL) or batroxobin (Pentapharm Ltd., Basel, Switzerland, 0.5 U/mL) was mixed with 90 μL of fibrinogen (0.20 mg/mL) in 20 mM N-[2-hydroxyethyl] piperazine-N'-[2-ethansulfonic acid] pH 7.4, 0.12 M NaCl (HEPES-buffered saline; HBS) added 1 mM $CaCl_2$. Three parameters: lag time, maximum slope (Vmax), and absorbance-change at 30-minute (ΔAbs_{30min}), were obtained from the turbidity curves as described previously [15]. Reactions were performed in triplicate for each sample.

Kinetics of FpA and FpB release

Fibrinopeptides release by thrombin or batroxobin was examined using reverse-phase high-performance liquid chromatography (HPLC) as described previously [10], with a few minor modifications. The final concentration in HBS of the sample preparation was as follow: thrombin: 0.05 U/mL or 4.0 U/mL or batroxobin: 0.05 U/mL and fibrinogen: 0.36 mg/mL), and these samples incubated at ambient temperature for various incubation periods. In addition, we prepared each sample, which was incubated with 4.0 U/mL thrombin or 0.5 U/mL batroxobin at 37℃ for 2-hour and defined these samples as the maximum release in each fibrinogen. To calculate the percentage of fibrinopeptide release, the amount of FpA or FpB released from the maximum release sample of normal fibrinogen was taken as 100%.

Initial structure preparation for molecular dynamics simulation

The complex models between the FpA fragment (AαG6-V20), which is the structure around the region that interacts with the active site in thrombin [7], and human α-thrombin were prepared as follows. First, 500 docking models of wild-type (WT) FpA fragment were prepared using a crystal structure (1UCY: complex model between the FpA fragment and bovine thrombin) [16] using Modeller9.24 [17]. The missing residues of the FpA fragment in 1UCY (AαG6, G17-V20) were fixed, and human thrombin was modeled using a bovine thrombin structure in 1UCY as a template. We selected the model that had the lowest discrete optimized protein energy score [18] in WT FpA fragment–thrombin complexes where the carbonyl oxygen of the AαR16 residue was located near thrombin S195 Oγ. Next, initial structures of the variant complex model were prepared in the same manner using an initial structure of the WT FpA fragment–thrombin complex as a template. Finally, N- and C-terminal of each FpA fragment model were capped.

Molecular dynamics simulation

We performed MD simulation using GROMACS 5.1.5 [19] and used the CHARMM36 force field [20]. Before MD simulation, energy minimization of each complex model was performed using the steepest descent minimization in a vacuum, and the maximum force was

set to 1,000 kJ/(mol·nm). Then, a TIP3P water model [21] was used as the solvation system, which was generated as a triclinic box with a side of 1.4 nm such that the FpA fragment–thrombin complexes were covered appropriately with water molecules [21]. These systems were neutralized using Na and Cl ions. Energy minimization of each system was performed using the steepest descent minimization, and the maximum force was set to 1,000 kJ/(mol·nm). After energy minimization, position-restrained dynamics simulation (NVT and NPT) of each system was done at 300 K for 100 picosecond (ps) or 1 nanosecond (ns), respectively. Finally, production simulations of each system were conducted for 100 ns at 300 K and 1 bar using periodic boundary conditions. The coupling algorithm of temperature (300 K) and pressure (1 bar) of each system was maintained using V-rescale (a modified Berendsen thermostat temperature coupling method) and the Parrinello-Rahman pressure coupling method, respectively, as described previously [22]. All bonds containing hydrogen atoms were constrained using the linear constraint solver algorithm, and the electrostatic interactions were treated with the particle-mesh-Ewald (PME) method, as described previously [23]. The stability of FpA fragment–thrombin complex models was analyzed using root-mean-square deviation (RMSD) (Figure S1), and snapshots in the MD simulation trajectory were confirmed using PyMOL [24]. Three thousand snapshots of the MD simulation trajectory between 50 and 80 ns were used in the binding free energy calculation.

Binding free energy calculation and per-residue energy decomposition analysis

The binding free energies of complexes between each the FpA fragment and human thrombin were calculated and analyzed using 3,000 snapshots between 50 ns and 80 ns MD simulation trajectories using the molecular mechanics Poisson–Boltzmann surface area (MM-PBSA) approach [25]. This analysis was performed using the g_mmpbsa tool of GROMACS [26,27]. Per-residue energy decomposition analysis of the WT FpA fragment–thrombin complex was also performed using the g_mmpbsa tool [26,27].

Statistical analysis

The significance of differences in fibrin polymerization between normal and patient's fibrinogen were assessed using Welch's t-test. A difference was considered to be significant when the p value was <0.05.

Results

Coagulation screening tests and DNA sequence analysis

The patient was a 12-year-old Japanese boy with Vincent's angina. His laboratory data showed low functional fibrinogen concentration (0.94 g/L, reference interval: 1.80–3.50 g/L). However, the immunological fibrinogen concentration (1.98 g/L, reference interval: 1.80–3.50 g/L) was normal. PT and APTT were 15.0 sec (reference interval: 10.8–13.2 sec) and 45.0 sec

(reference interval: 23.0–38.0 sec), respectively. He and his family members had not experienced any episodes of abnormal bleeding or thrombosis. From DNA sequence analysis for exons (*FGA* exon 2 and 5, *FBG* exon 2, and *FGG* exon 8 and 9) and these exon-intron boundaries, the patient had a heterozygous variant with a three-nucleotide deletion (two A and one G) between *FGA* exon 2 c.87 and c.90 (*FGA* exon 2 c.88_90del), resulting in deletion of the AαE11 residue (mature protein) or Aαp.E30 (native protein) (AαE11del). This mutation was designated as fibrinogen Soka and was the first case in the world.

Characterization of purified plasma fibrinogens

Purified plasma fibrinogen was electrophoresed by SDS-PAGE under reducing condition (10% gel) and non-reducing condition (5% gel) and was observed by staining the protein with Coomassie Brilliant Blue R-250. In either condition, patient's fibrinogen showed the typical pattern, and it was confirmed that these samples were high purity (data not shown).

Thrombin- or batroxobin-catalyzed fibrin polymerization

The turbidity curves and three parameters are shown in Figure 1 and Table 1, respectively. Thrombin catalyzed fibrin polymerization (TCFP) catalyzed with 0.05 U/mL thrombin for patient's fibrinogen was impaired: lag time of patient's fibrinogen was 5.3 min longer than that of normal fibrinogen and maximum slope (Vmax) of the former was 21% of the latter (Figure

1A). On the other hand, TCFP with 4.0 U/mL thrombin for the variant was improved more than TCFP with 0.05 U/mL thrombin for the variant: Vmax of patient's fibrinogen with 4.0 U/mL thrombin improved to 41% of normal fibrinogen with 4.0 U/mL thrombin. (Figure 1B). Furthermore, batroxobin-catalyzed fibrin polymerization (BCFP) catalyzed with 0.05 U/mL batroxobin for patient's fibrinogen was slightly impaired: Vmax of the variant fibrinogen was 75% of normal fibrinogen (Figure 1C).

Kinetics of FpA and FpB release

FpA and FpB release kinetics were analyzed using reverse-phase HPLC. We incubated each fibrinogen with 4.0 U/mL thrombin or 0.5 U/mL batroxobin at 37°C for 2 hours (maximum release conditions), and these chromatograms are shown in Figure 2. The WT amino acid sequence of each peak are shown in Table 2 [28]. Patient's fibrinogen showed variant FpA peaks in either condition (Figure 2A, B). These variant FpA peaks areas were almost the same as normal FpA peaks areas.

Next, we observed the kinetics of FpA and FpB release from each fibrinogen with 0.05 U/mL or 4.0 U/mL thrombin or 0.05 U/mL batroxobin. With 0.05 U/mL thrombin catalyzation, total FpA release (sum of normal FpA and variant FpA) from patient's fibrinogen (heterozygous patient) were approximately 50% of that from normal fibrinogen, namely variant FpA was slightly released from patient's fibrinogen (Figure 3A). FpB release from variant fibrinogen

was almost the same as normal fibrinogen (Figure 3B). Moreover, with 4.0 U/mL thrombin catalyzation, variant FpA release was increased from patient's fibrinogen (Figure 3C). On the other hand, with 0.05 U/mL batroxobin catalyzation, variant FpA release from patient's fibrinogen was increased much more than with 0.05 U/mL thrombin catalyzation (Figure 3A, D).

Molecular dynamics simulation, binding free energy calculation, and energy decomposition analysis

MD simulation of WT or AαE11del FpA fragment (AαG6-V20)–thrombin complex was performed until 100 ns using GROMACS software [19].

Using the trajectory obtained from the MD simulation, the binding free energy of each FpA fragment–thrombin complex was calculated using the MM-PBSA method [25]. Because the binding free energy shows the strength of the binding between protein and ligand, minus and larger absolute values indicate a more stable structure of the complex. The binding free energy of WT FpA fragment–thrombin complex was -46.98 ± 9.31 kcal/mol and a more negative value than AαE11del FpA fragment–thrombin complex (-30.95 ± 8.14 kcal/mol). Thus, the AαE11del FpA fragment–thrombin complex was more unstable than the WT FpA fragment–thrombin complex.

To identify the important residues in FpA related to the binding process into thrombin, the binding free energy of the WT FpA fragment–thrombin complex was decomposed into the contribution of each residue. This finding indicated that larger residues showed negative energy, and the more this residue contributes to produce low overall binding free energy. As shown in Figure 4, the AαE11 residue was the highest contributor (-7.56 kcal/mol) among WT FpA fragment residues. The contribution of other residue was decreased in the order AαD7 (-6.91 kcal/mol), AαF8 (-6.03 kcal/mol), AαP18 (-3.85 kcal/mol), and AαV15 (-3.78 kcal/mol).

Discussion

We identified a heterozygous AαE11del variant with congenital dysfibrinogenemia and designated it as fibrinogen Soka. This amino acid deletion was the first case in the world. Another variant fibrinogen at this position, fibrinogen Mitaka II (heterozygous AαE11G), has been reported as dysfibrinogenemia [29].

In 0.05 U/mL thrombin, the FpA release from the WT Aα chain in the patient's fibrinogen was normal, but variant FpA release was significantly reduced. Thus, TCFP catalyzed with 0.05 U/mL thrombin for patient's fibrinogen was impaired due to the reduction in variant FpA release from the variant fibrinogen. However, TCFP catalyzed with 4.0 U/mL thrombin for patient's fibrinogen was improved by reflecting the increase in variant FpA release. Conversely, BCFP catalyzed with 0.05 U/mL batroxobin for patient's fibrinogen was similar to that of

normal fibrinogen, because FpA release from patient's fibrinogen was almost as normal with 0.05 U/mL batroxobin. Moreover, fibrinogen Mitaka II (AαE11G) showed properties similar to fibrinogen Soka (AαE11del): polymerization by thrombin was prolonged, but that with snake venom protease, ancrod, was normal [29]. Namely, these results suggested that the AαE11 residue might be more associated with thrombin catalyzation than FpA cleavage by snake venom protease catalyzation such as with batroxobin and ancrod.

To clarify the association between the AαE11 residue and thrombin, the binding free energy of FpA fragment–thrombin complex was analyzed. These results indicated that the AαE11del FpA fragment–thrombin complex was more unstable than the WT FpA fragment–thrombin complex. Furthermore, for fibrinogen Mitaka II it has been reported that thrombin binding was approximately 50% of normal fibrinogen using ^{125}I-labeled diisopropyl-thrombin [29]. Then, we prepared a AαE11G FpA fragment–thrombin complex model and calculated its binding free energy in the same manner. As a result, the binding free energy of the AαE11G FpA fragment–thrombin complex was -32.73 ± 10.34 kcal/mol, indicating that it was more unstable than the WT FpA fragment–thrombin complex as with the AαE11del FpA fragment–thrombin complex (-30.95 ± 8.14 kcal/mol). Moreover, inside the WT FpA fragment, the AαE11 residue contributed most to the complex stabilization between the WT FpA fragment and thrombin. Other residues that showed higher contribution in the complex stabilization were residues AαD7 and AαF8. Variant fibrinogens at these residues were reported as fibrinogen

Lille (AαD7N) and fibrinogen United Kingdom (AαF8C) [30,31], respectively. Similar to the AαE11del and AαE11G mutations, fibrinogen Lille demonstrated delayed FpA release [30]. However, fibrinogen United Kingdom has not been analyzed for FpA release, but thrombin time was prolonged [31]. Of interest, mutations located outside of the FpA cleavage site (AαR16-G17) related to FpA release levels.

As mentioned above, we demonstrated that the AαE11 residue contributes to the stabilization between thrombin and the FpA fragment (AαG6-V20) and is required for efficient FpA release. Additionally, focusing on FpA structure, Martin et al. demonstrated that AαD7-E11 residues form one turn of a helix, and AαL9-G12 residues form a type I β-turn [9], namely, the AαE11 residue is a component of both structures. In experiments using synthetic peptides and thrombin, the kinetic constants between peptide and thrombin using the AαG13-R23 peptide and AαA10-R23 peptide were lower than with the AαF8-R23 peptide (complete form type I β-turn: AαL9-G12), namely the kinetic constant was 80-fold more than when an AαA10-R23 peptide was used [32]. In addition, the kinetic constant using an AαD7-V20 peptide (complete form one helix turn: AαD7-E11, and type I β-turn: AαL9-G12) was 3.1-fold more than when an AαF8-V20 peptide was used [33,34]. Finally, these secondary structures were related to FpA release from fibrinogen.

Moreover, not only these FpA structures but also the binding between thrombin and FpA has been reported to play a key role in FpA release from fibrinogen, and this binding is the salt

bridge between the thrombin R173 residue and AαE11 residue [35]. Thus, there is a possibility that FpA structures (one helix turn and type I β-turn) and this salt bridge are needed for stable complex structure formation and efficient FpA release. Moreover, both deletion and mutation at the AαE11 residue destabilized FpA-thrombin binding and impaired FpA release by breaking these structures and the salt bridge.

In conclusion, this study demonstrated that the AαE11 residue plays a more important role in FpA release with thrombin catalyzation than with batroxobin catalyzation. Moreover, the AαE11 residue contributed to the binding stability of the FpA fragment and thrombin complex.

Authorship

Takahiro Kaido and Masahiro Yoda performed the research and analyzed the data. T. Kaido wrote the manuscript. Tomu Kamijo, Shinpei Arai, Kazuyoshi Yamauchi, and Nobuo Okumura designed the research and discussed the data. N. Okumura and S. Arai reviewed the manuscript.

Declaration of competing interest

The authors state that they have no conflicts of interest.

Acknowledgment

We gratefully acknowledge Dr. Takeshi Sato (Soka Municipal Hospital, Soka, Saitama), for the patient referral. This work was supported by JSPS KAKENHI Grant Number JP20K07799 (Nobuo Okumura).

References

1. Weisel JW. Fibrinogen and fibrin. Adv Protein Chem. United States; 2005;70:247–99.

2. Weisel JW, Litvinov RI. Fibrin Formation, Structure and Properties. Subcell Biochem. 2017;82:405–56.

3. Huang S, Cao Z, Chung DW, Davie EW. The role of betagamma and alphagamma complexes in the assembly of human fibrinogen. J Biol Chem. United States; 1996;271:27942–7.

4. Medved L, Weisel JW, Haemostasis F and FXS of SSC of IS on T and. Recommendations for nomenclature on fibrinogen and fibrin. J Thromb Haemost. 2009;7:355–9.

5. Blombäck B, Hessel B, Hogg D, Therkildsen L. A two-step fibrinogen-fibrin transition in blood coagulation. Nature. England; 1978;275:501–5.

6. Aronson DL. Comparison of the actions of thrombin and the thrombin-like venom enzymes ancrod and batroxobin. Thromb Haemost. Germany; 1976;36:9–13.

7. Rose T, Di Cera E. Three-dimensional modeling of thrombin-fibrinogen interaction. J Biol Chem. United States; 2002;277:18875–80.

8. Groupe d'etude sur l'hemostase et la thrombose. Human fibrinogen database release 50 [Internet]. 2020 [cited 2020 Aug 31]. Available from: https://site.geht.org/base-de-donnees-fibrinogene/.

9. Martin PD, Robertson W, Turk D, Huber R, Bode W, Edwards BF. The structure of residues 7-16 of the A alpha-chain of human fibrinogen bound to bovine thrombin at 2.3-A resolution. J Biol Chem. United States; 1992;267:7911–20.

10. Kaido T, Yoda M, Kamijo T, Taira C, Higuchi Y, Okumura N. Comparison of molecular structure and fibrin polymerization between two Bβ-chain N-terminal region fibrinogen variants, Bβp.G45C and Bβp.R74C. Int J Hematol. Japan; 2020;112:331–40.

11. Terasawa F, Okumura N, Kitano K, Hayashida N, Shimosaka M, Okazaki M, et al. Hypofibrinogenemia Associated With a Heterozygous Missense Mutation γ153Cys to Arg (Matsumoto IV): In Vitro Expression Demonstrates Defective Secretion of the Variant Fibrinogen. Blood. United States; 1999;94:4122–31.

12. Takebe M, Soe G, Kohno I, Sugo T, Matsuda M. Calcium ion-dependent monoclonal antibody against human fibrinogen: preparation, characterization, and application to fibrinogen purification. Thromb Haemost. Germany; 1995;73:662–7.

13. Gorkun O V, Veklich YI, Weisel JW, Lord ST. The conversion of fibrinogen to fibrin: recombinant fibrinogen typifies plasma fibrinogen. Blood. United States; 1997;89:4407–14.

14. Mihalyi E. Physicochemical studies of bovine fibrinogen. IV. Ultraviolet absorption and its relation to the structure of the molecule. Biochemistry. United States; 1968;7:208–23.

15. Ikeda M, Kobayashi T, Arai S, Mukai S, Takezawa Y, Terasawa F, et al. Recombinant γT305A fibrinogen indicates severely impaired fibrin polymerization due to the aberrant

function of hole “A” and calcium binding sites. Thromb Res. United States; 2014;134:518–25.

16. Martin PD, Malkowski MG, DiMaio J, Konishi Y, Ni F, Edwards BF. Bovine thrombin complexed with an uncleavable analog of residues 7-19 of fibrinogen A alpha: geometry of the catalytic triad and interactions of the P1’, P2’, and P3’ substrate residues. Biochemistry. United States; 1996;35:13030–9.

17. Sali A, Blundell TL. Comparative protein modelling by satisfaction of spatial restraints. J Mol Biol. England; 1993;234:779–815.

18. Shen M-Y, Sali A. Statistical potential for assessment and prediction of protein structures. Protein Sci. 2006;15:2507–24.

19. Abraham MJ, Murtola T, Schulz R, Páll S, Smith JC, Hess B, et al. GROMACS: High performance molecular simulations through multi-level parallelism from laptops to supercomputers. SoftwareX. 2015;1–2:19–25.

20. Best RB, Zhu X, Shim J, Lopes PEM, Mittal J, Feig M, et al. Optimization of the additive CHARMM all-atom protein force field targeting improved sampling of the backbone φ, ψ and side-chain χ(1) and χ(2) dihedral angles. J Chem Theory Comput. 2012;8:3257–73.

21. Jorgensen WL, Chandrasekhar J, Madura JD, Impey RW, Klein ML. Comparison of simple potential functions for simulating liquid water. J Chem Phys. 1983;79:926–35.

22. Pandey B, Grover A, Sharma P. Molecular dynamics simulations revealed structural differences among WRKY domain-DNA interaction in barley (Hordeum vulgare). BMC Genomics. 2018;19:132.

23. Yu H, Wang M, Xuan N, Shang Z, Wu J. Molecular dynamics simulation of the interactions between EHD1 EH domain and multiple peptides. J Zhejiang Univ Sci B. 2015;16:883–96.

24. Schrödinger L. The PyMOL Molecular Graphics System, Version 2.0. 2015.

25. Kollman PA, Massova I, Reyes C, Kuhn B, Huo S, Chong L, et al. Calculating structures and free energies of complex molecules: combining molecular mechanics and continuum models. Acc Chem Res. United States; 2000;33:889–97.

26. Kumari R, Kumar R, Lynn A. g_mmpbsa—A GROMACS Tool for High-Throughput MM-PBSA Calculations. J Chem Inf Model. American Chemical Society; 2014;54:1951–62.

27. Baker NA, Sept D, Joseph S, Holst MJ, McCammon JA. Electrostatics of nanosystems: Application to microtubules and the ribosome. Proc Natl Acad Sci. 2001;98:10037 LP – 10041.

28. Kehl M, Lottspeich F, Henschen A. Analysis of human fibrinopeptides by high-performance liquid chromatography. Hoppe Seylers Z Physiol Chem. Germany; 1981;362:1661–4.

29. Niwa K, Yaginuma A, Nakanishi M, Wada Y, Sugo T, Asakura S, et al. Fibrinogen Mitaka II: a hereditary dysfibrinogen with defective thrombin binding caused by an A alpha Glu-11 to Gly substitution. Blood. United States; 1993;82:3658–63.

30. Denninger MH, Finlayson JS, Reamer LA, Parquet-Gernez A, Goudemand M, Menache D. Congenital dysfibrinogenemia: fibrinogen Lille. Thromb Res. United States; 1978;13:453–66.

31. Shapiro SE, Phillips E, Manning RA, Morse C V, Murden SL, Laffan MA, et al. Clinical phenotype, laboratory features and genotype of 35 patients with heritable dysfibrinogenaemia. Br J Haematol. England; 2013;160:220–7.

32. van Nispen JW, Hageman TC, Scheraga HA. Mechanism of action of thrombin on fibrinogen. The reaction of thrombin with fibrinogen-like peptides containing 11, 14, and 16 residues. Arch Biochem Biophys. United States; 1977;182:227–43.

33. Meinwald YC, Martinelli RA, van Nispen JW, Scheraga HA. Mechanism of action of thrombin on fibrinogen. Size of the A alpha fibrinogen-like peptide that contacts the active site of thrombin. Biochemistry. United States; 1980;19:3820–5.

34. Marsh HCJ, Meinwald YC, Thannhauser TW, Scheraga HA. Mechanism of action of thrombin on fibrinogen. Kinetic evidence for involvement of aspartic acid at position P10. Biochemistry. United States; 1983;22:4170–4.

35. Stubbs MT, Oschkinat H, Mayr I, Huber R, Angliker H, Stone SR, et al. The interaction of thrombin with fibrinogen. A structural basis for its specificity. Eur J Biochem. England; 1992;206:187–95.

Figure legends

Fig. 1

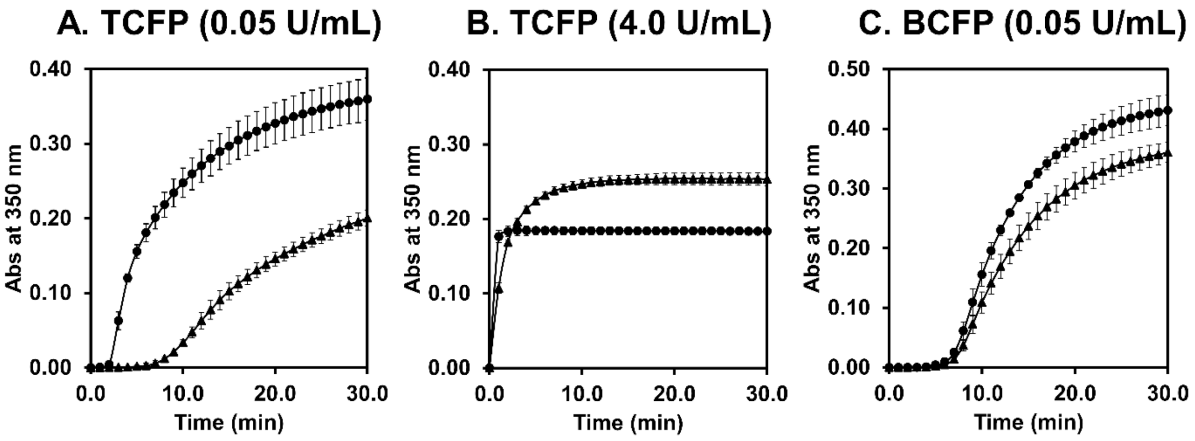

Figure 1. Thrombin- or batroxobin-catalyzed fibrin polymerization. Fibrin polymerization was performed in following conditions; thrombin: 0.05 U/mL (Panel A) or 4.0 U/mL (Panel B), batroxobin: 0.05 U/mL (Panel C), fibrinogen: 0.18 mg/mL, $CaCl_2$: 1 mM. Data are presented as mean ± S.D.. TCFP: thrombin-catalyzed fibrin polymerization, BCFP: batroxobin-catalyzed fibrin polymerization. Normal fibrinogen (closed circle), patient's fibrinogen (closed triangle).

Fig. 2

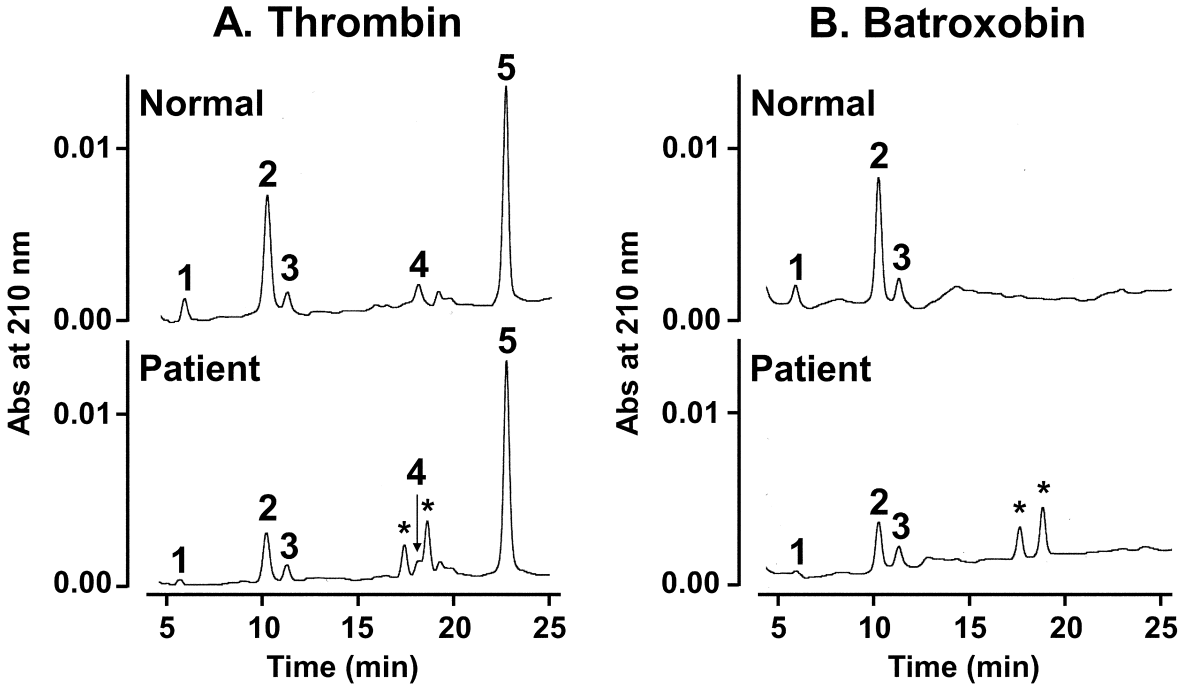

Figure 2. Chromatograms of thrombin- or batroxobin-induced fibrinopeptide release. Each panel showed chromatograms of reverse-phase HPLC for sample after a 2-hour incubation with thrombin (4.0 U/mL; Panel A) or batroxobin (0.5 U/mL; Panel B) at 37°C. Each peak is shown as follow; FpA: AP (1), A (2), and AY (3), FpB: des-Arg-B (4) and B (5), and these amino acid sequences are shown in Table 2 [28]. *: variant FpA.

Fig.3

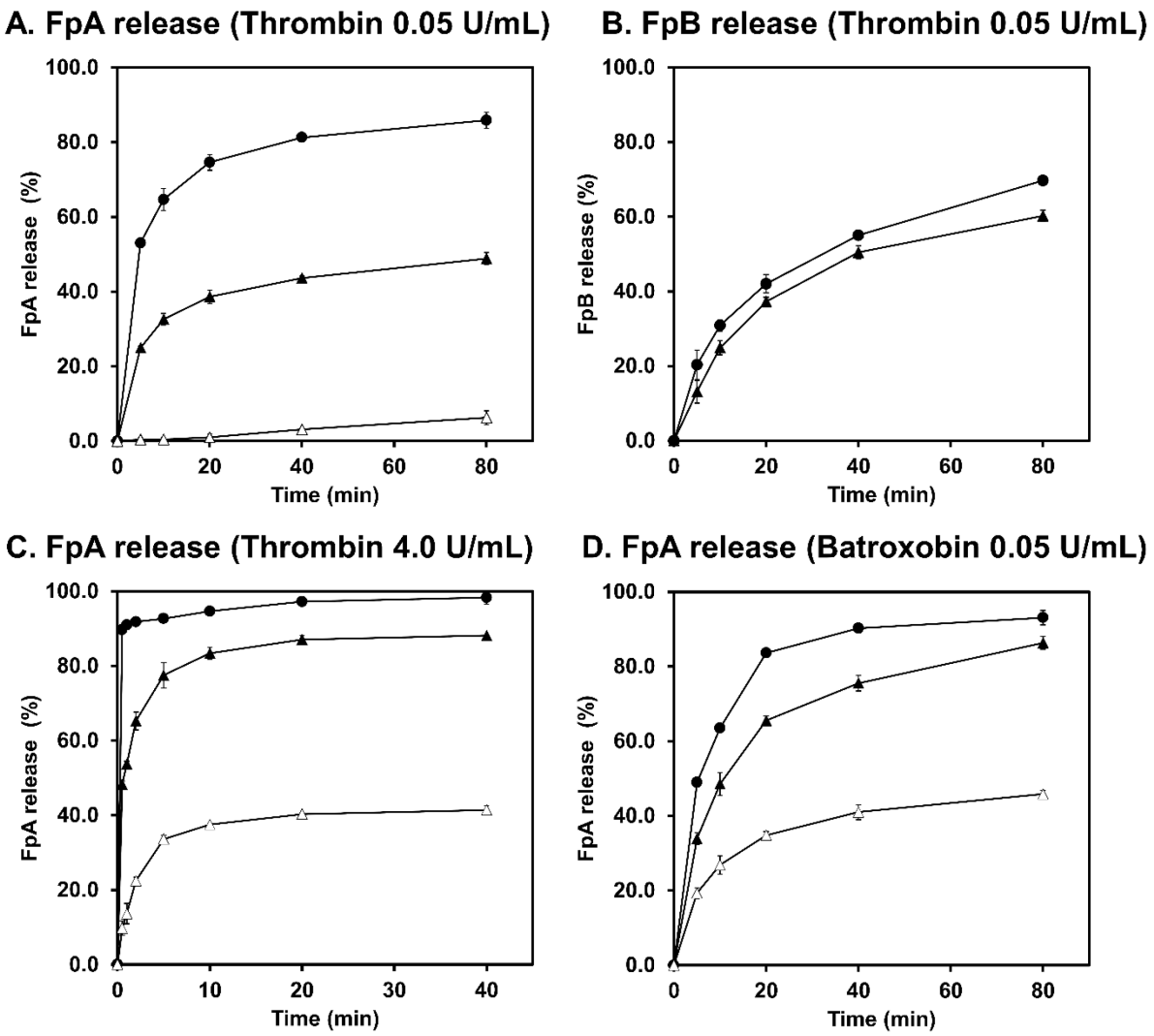

Figure 3. Kinetics of FpA and FpB release. 0.05 U/mL thrombin-induced FpA and FpB release (Panels A and B), 4.0 U/mL thrombin-induced FpA release (Panel C), and 0.05 U/mL batroxobin-induced FpA release (Panel D) from purified normal and patient's fibrinogens were determined using reverse-phase HPLC. The percentage of FpA and FpB release was calculated versus that of normal fibrinogen after a 2-hour incubation with thrombin (4.0 U/mL) or batroxobin (0.5 U/mL) at 37℃ as 100%. Each panel showed FpA or FpB release from normal

fibrinogen (circle) and patient's fibrinogen (triangle). Closed and open symbols show total release and variant FpA release, respectively. Data are presented as mean ± S.D..

Fig. 4

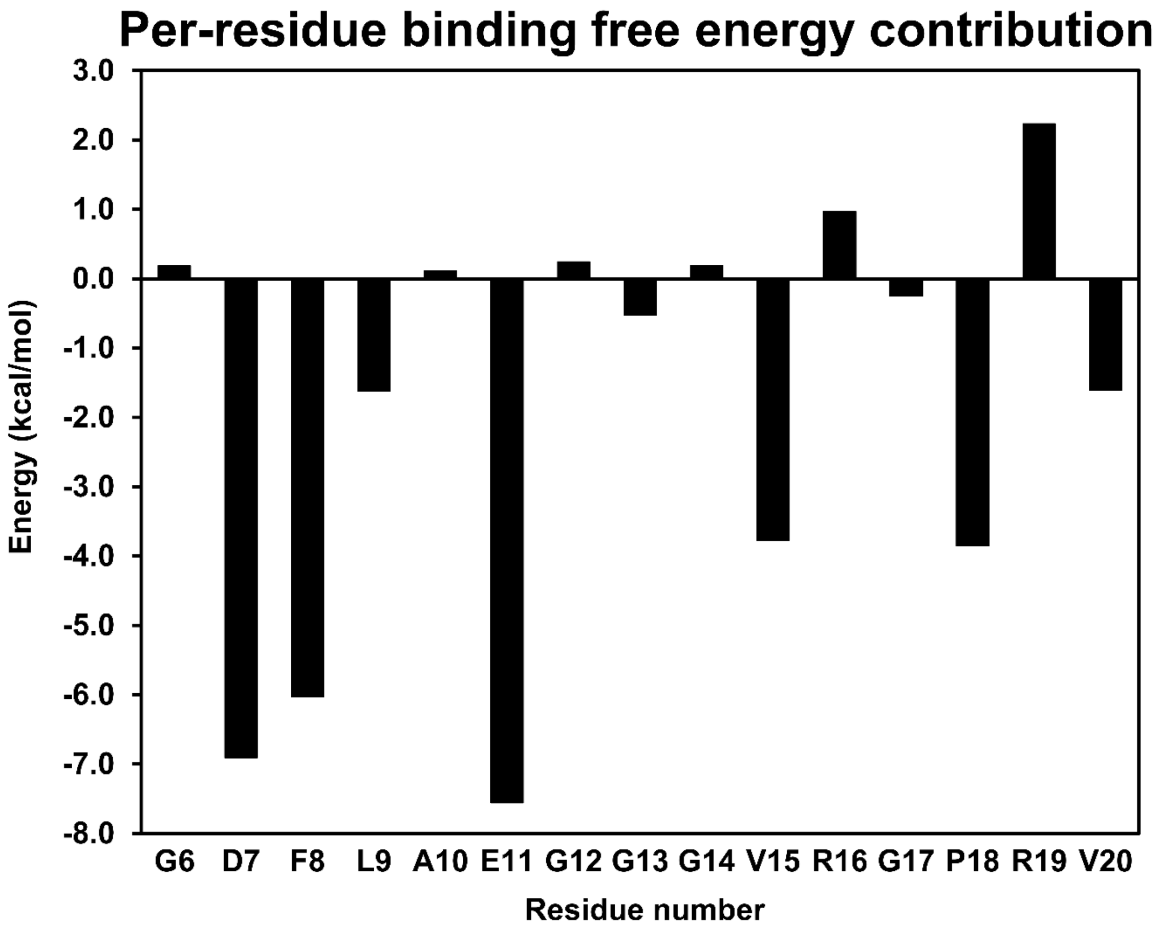

Figure 4. Per-residue binding free energy contribution of the wild-type FpA fragment–thrombin complex. The binding free energy of wild-type (WT) FpA fragment–thrombin complex was decomposed into the contribution of each residue, out of which energies of WT FpA fragment residues are shown. The lower energy of these residues contributes to the stability of the complex.

Supplementary Figure 1. The root-mean-square deviation of each complex model backbone atoms in the 100 ns MD simulation trajectory. The root-mean-square deviation (RMSD) of each FpA fragment–thrombin heavy chain complex was measured by its deviation from each initial structure. RMSDs of wild-type or AαE11del FpA fragment–thrombin complex models are indicated by black and red, respectively.

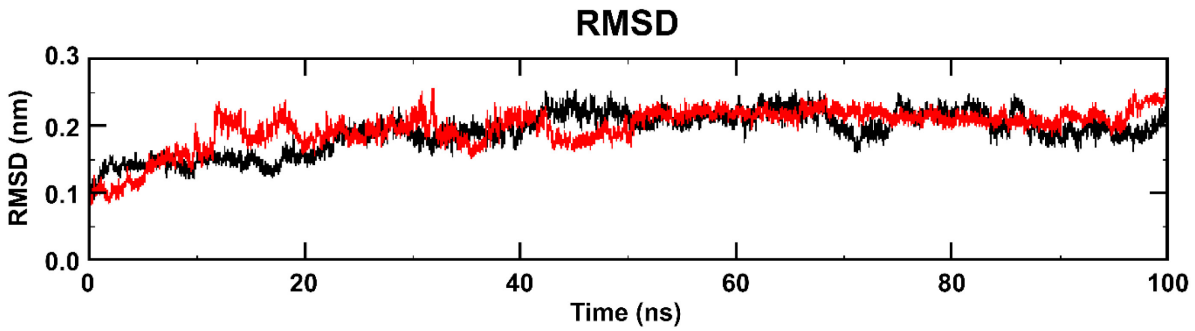

Table legends

	Normal	Patient
TCFP (0.05 U/mL)		
Lag time (min)	2.0 ± 0.15	7.3 ± 0.17***
Vmax ($\times 10^{-4}$/sec)	12.1 ± 0.20	2.5 ± 0.34***
ΔAbs_{30min}	0.360 ± 0.028	0.201 ± 0.012***
TCFP (4.0 U/mL)		
Lag time (min)	0.2 ± 0.00	0.3 ± 0.06*
Vmax ($\times 10^{-4}$/sec)	73.8 ± 9.92	30.1 ± 3.17***
ΔAbs_{30min}	0.183 ± 0.005	0.253 ± 0.009***
BCFP (0.05 U/mL)		
Lag time (min)	5.8 ± 0.31	6.5 ± 0.12*
Vmax ($\times 10^{-4}$/sec)	8.3 ± 0.51	6.2 ± 0.84*
ΔAbs_{30min}	0.432 ± 0.027	0.361 ± 0.017*

Table 1: Parameters of thrombin- or batroxobin-catalyzed fibrin polymerization. Data are presented as mean ± S.D. with three experiments in each condition. The statistical analysis between normal fibrinogen and patient's fibrinogen was performed using Welch's t-test. *p**: <0.05, *p****: <0.001. TCFP: thrombin-catalyzed fibrin polymerization, BCFP: batroxobin-catalyzed fibrin polymerization, ΔAbs30min: absorbance change at 30 minutes.

		Sequence
FpA	AP	(1) A D S_P G E G D F L A E G G G V R (16)
	A	(1) A D S G E G D F L A E G G G V R (16)
	AY	(2) – D S G E G D F L A E G G G V R (16)
FpB	des-Arg-B	(1) Z G V N D N E E G F F S A – (13)
	B	(1) Z G V N D N E E G F F S A R (14)

Table 2: Amino acid sequences of normal fibrinopeptide A and B. Amino acid sequences were showed by one letter. In AαE11del variant, the amino acid shown by underline was deleted. FpA: fibrinopeptide A, FpB: fibrinopeptide B, S_P: phosphoserine, –: deletion of amino acid, Z: pyroglutamic acid. The number in parenthesis shows the first and last amino acid number of each peptide.